Image Cover Sheet

CLASSIFICATION	SYSTEM NUMBER
UNCLASSIFIED	510311

TITLE

FRACTURE TOUGHNESS OF STEEL WELDMENTS AT HIGH LOADING RATES

System Number:

Patron Number:

Requester:

Notes: Paper #6 contained in Parent Sysnum #510305

DSIS Use only:

Deliver to: DK

#510311 (6)

FRACTURE TOUGHNESS OF STEEL WELDMENTS AT HIGH LOADING RATES

by

M.N. Bassim* and J.R. Matthews**

* Department of Mechanical and Industrial Engineering, University of Manitoba, Winnipeg, Manitoba, Canada R3T 2N2

** Defence Research Establishment Atlantic, Dockyard Laboratory, FMO Halifax, Nova Scotia, Canada B3K 2XO

ABSTRACT

Fracture toughness for a number of submarine hull steels and steel weldments was determined at very high rates of loading, in excess of strain rates of 10^3 s^{-1}, corresponding to loading rates of $\dot{K}$ larger than 10^6 MPa $m^{1/2}$ s^{-1} using a modified version of a Split Hopkinson pressure bar equipped with a swing arm mechanism. The parameter J_{IC} was determined from measurement of the stretch zone width (SZW) using scanning electron microscopy on the fractured specimens. The impact tests were performed on compact tension specimens at -30°C. Concurrently, two studies, one involving impact testing at slower velocities using a drop-weight tester and the other relating the measured SZW to the fatigue prestraining, were conducted. It was found that, while prestraining has a significant effect on the SZW, there are no significant differences in the SZW between using a nine-point approach, (ASTM) and a three point approach for very high strain rates.

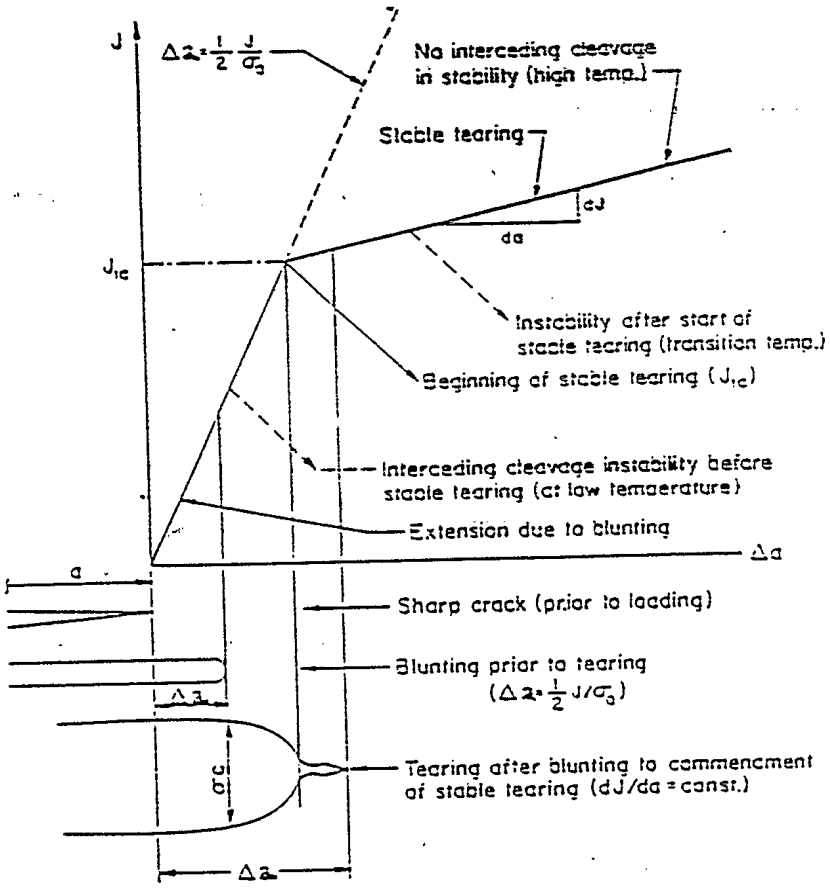

Figure 1: The relationship between J integral and Δa.

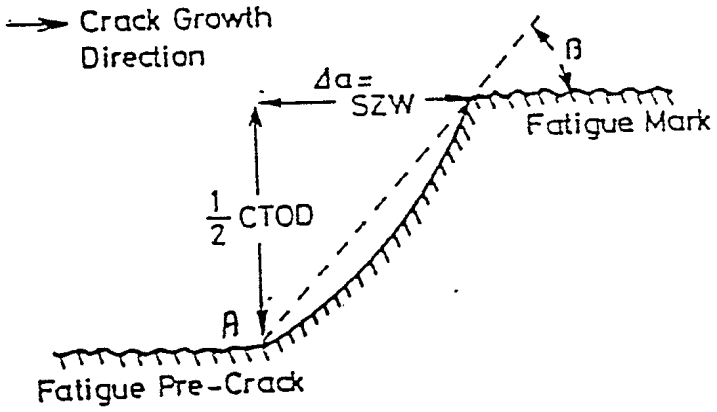

Figure 2: Schematic section profile of stretch zone.

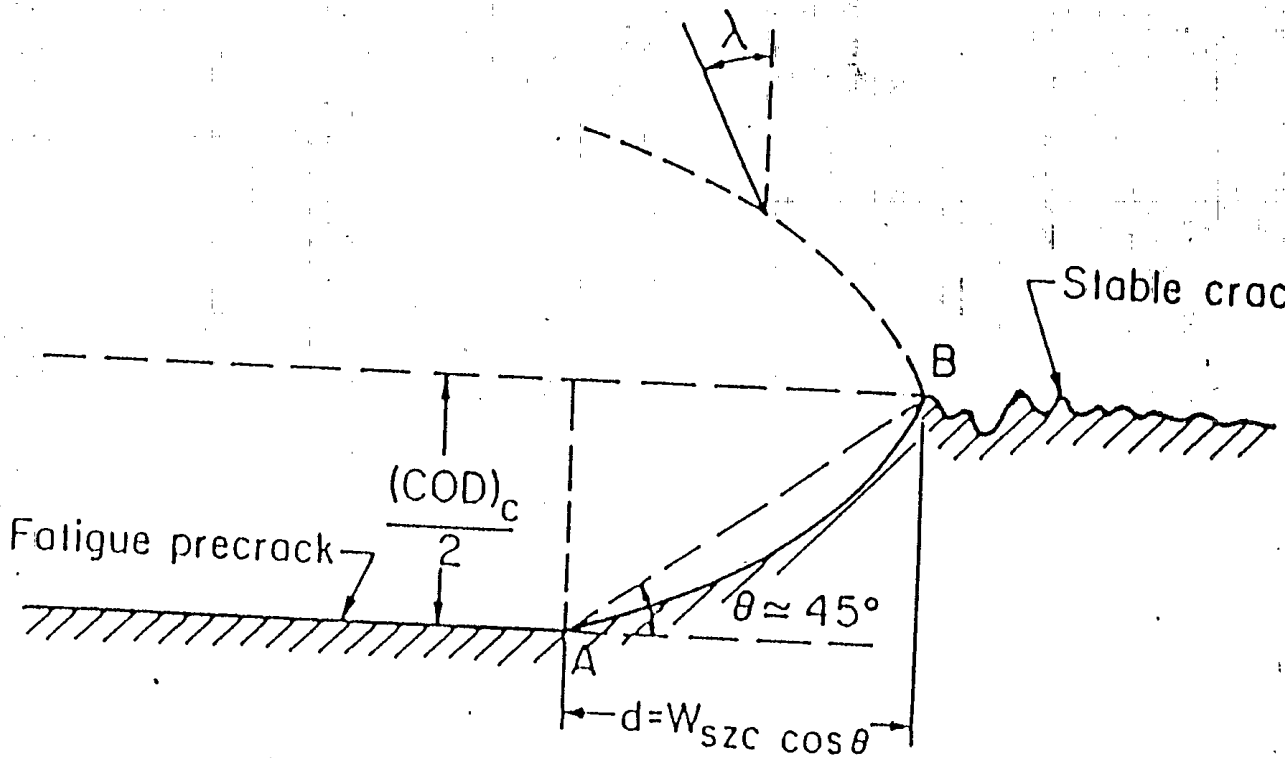

FIG 1. CONCEPT OF THE STRETCH ZONE APPROACH

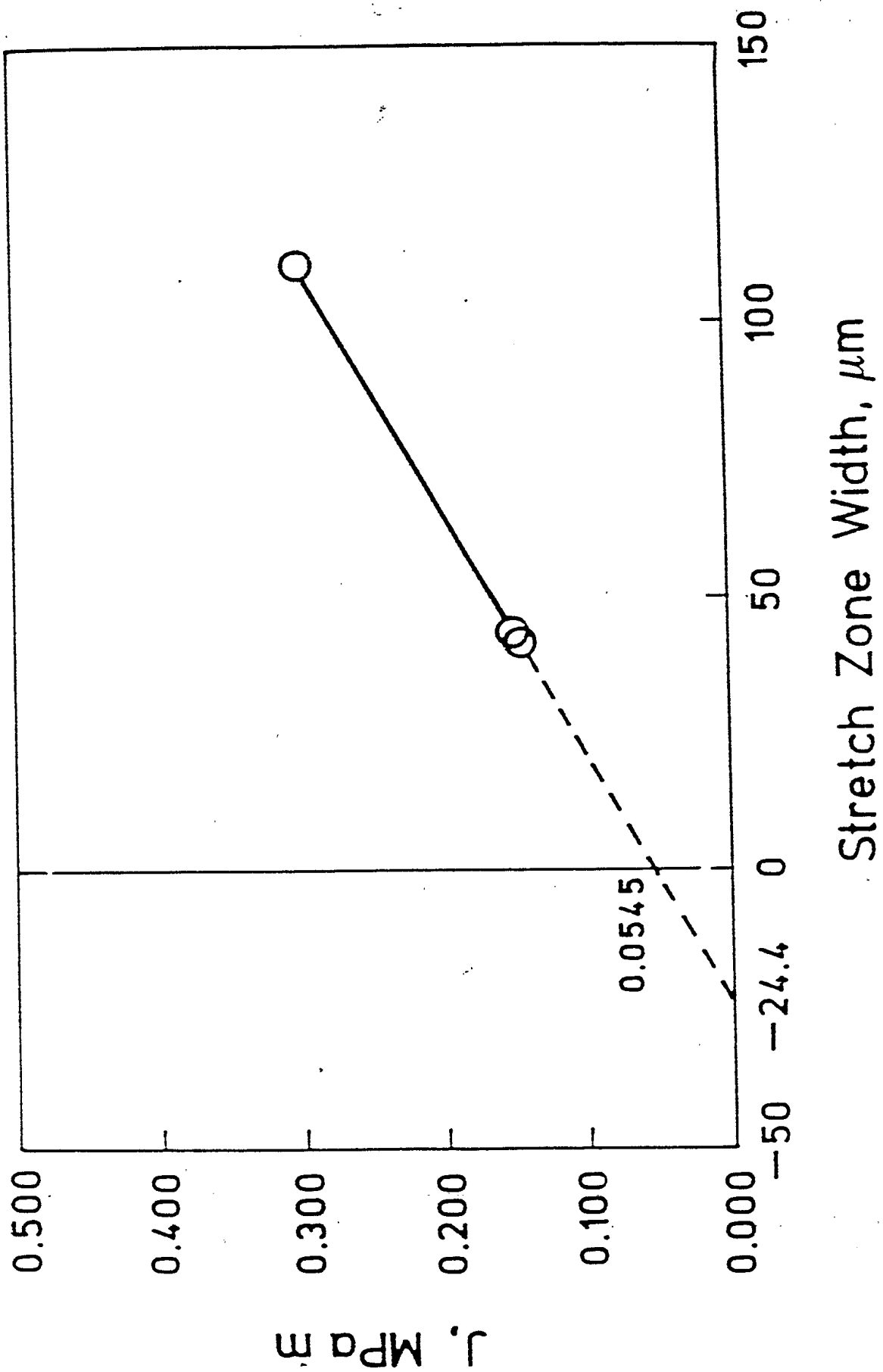
J, MPa m
0.500
0.400
0.300
0.200
0.100
0.000
0.0545
−50
−24.4
0
50
100
150
Stretch Zone Width, μm

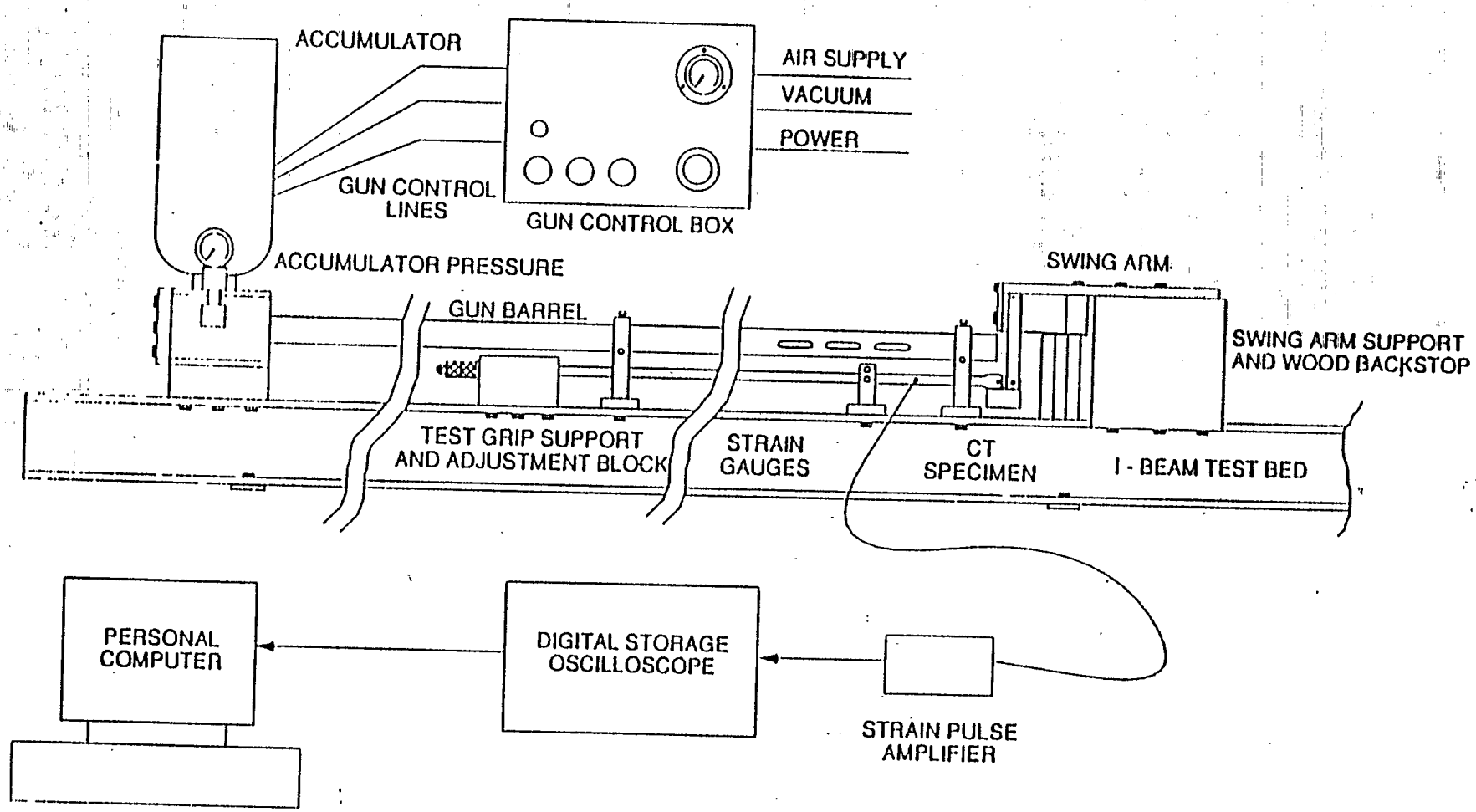
ACCUMULATOR
AIR SUPPLY
VACUUM
POWER
GUN CONTROL LINES
GUN CONTROL BOX
ACCUMULATOR PRESSURE
SWING ARM
GUN BARREL
SWING ARM SUPPORT AND WOOD BACKSTOP
TEST GRIP SUPPORT AND ADJUSTMENT BLOCK
STRAIN GAUGES
CT SPECIMEN
I - BEAM TEST BED
PERSONAL COMPUTER
DIGITAL STORAGE OSCILLOSCOPE
STRAIN PULSE AMPLIFIER

Fig 2

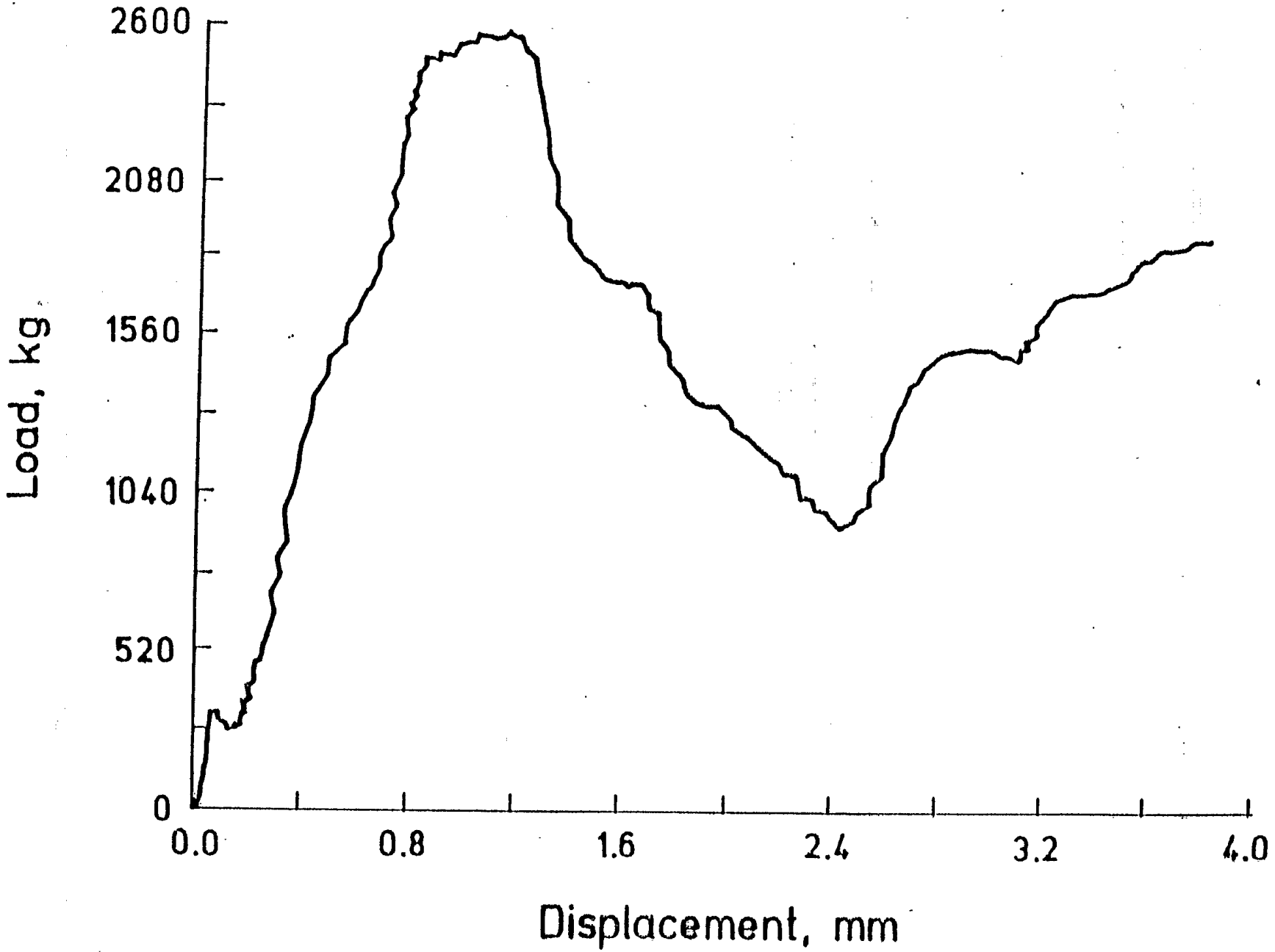
2600
2080
1560
1040
520
0
Load, kg
0.0
0.8
1.6
2.4
3.2
4.0
Displacement, mm

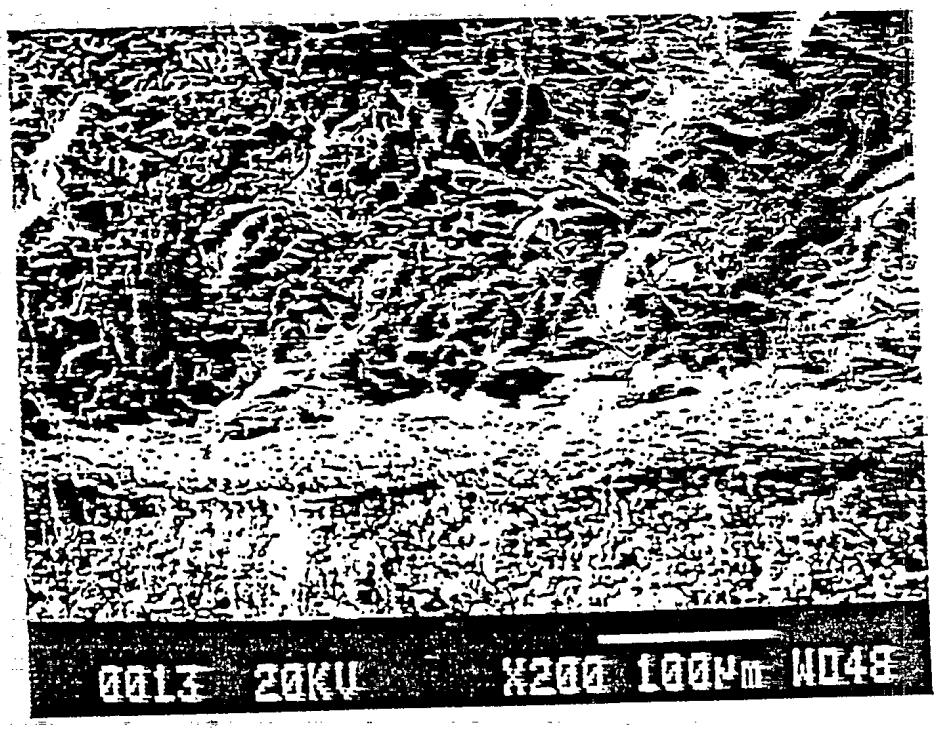

(a)

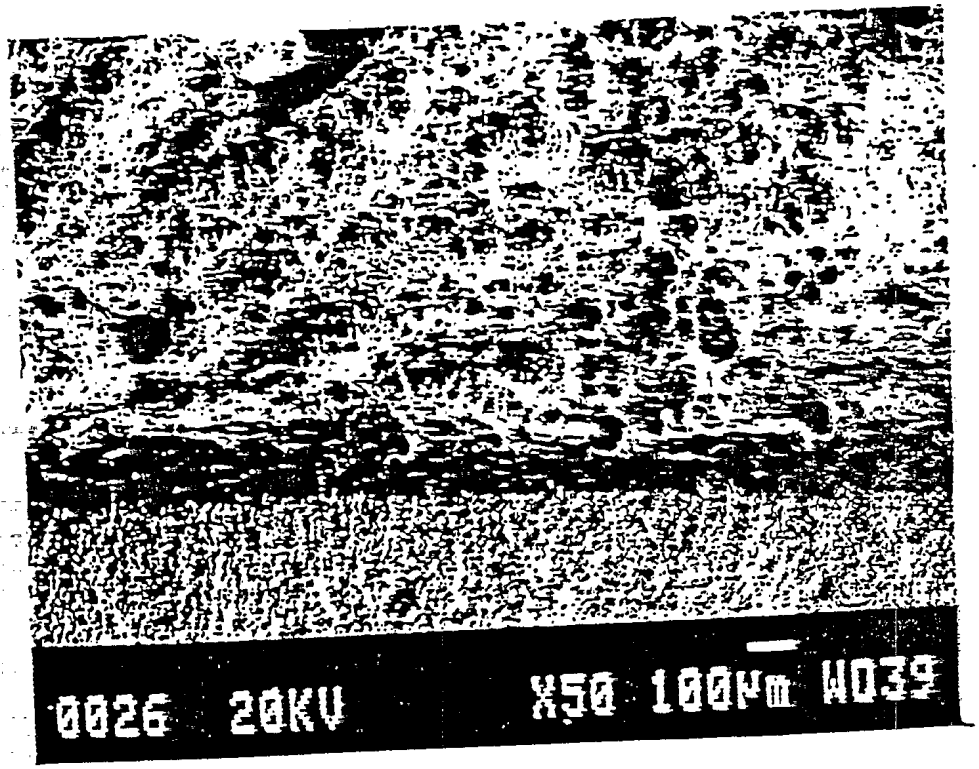

(b)

FIG.17: Stretch zone width micrographs of (a) QS1 and (b) SHB5 specimen

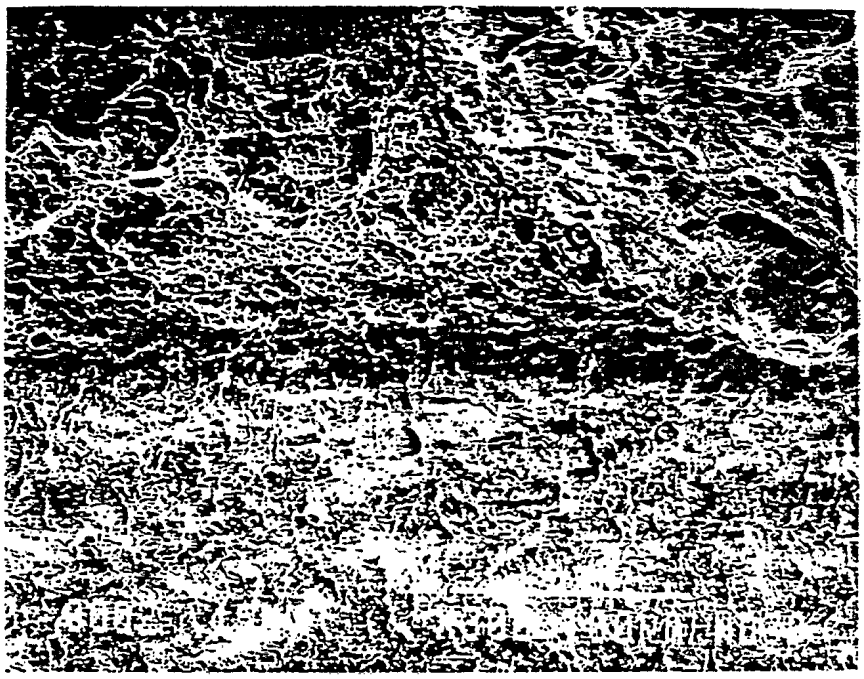

(a)

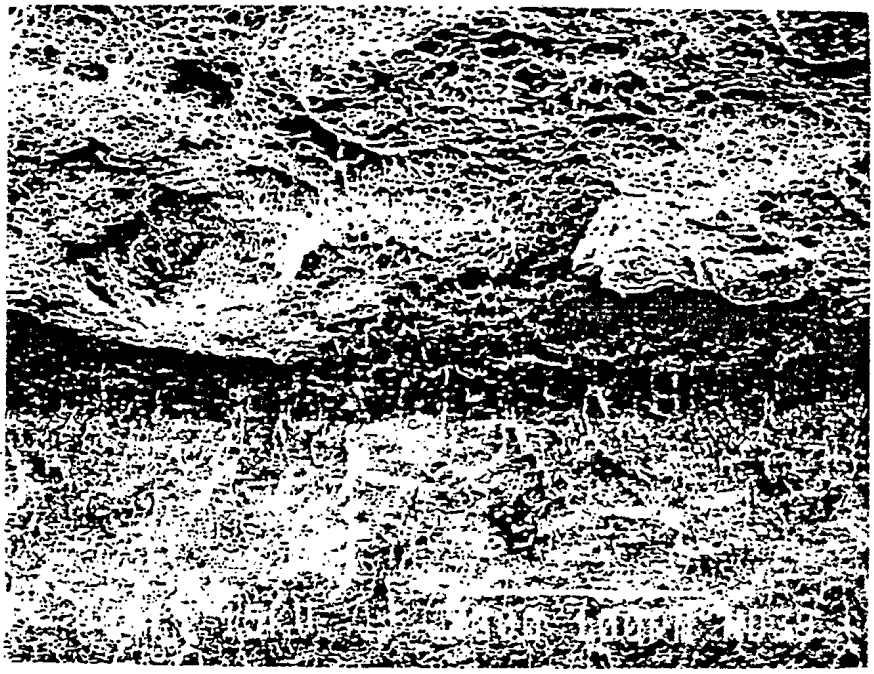

(b)

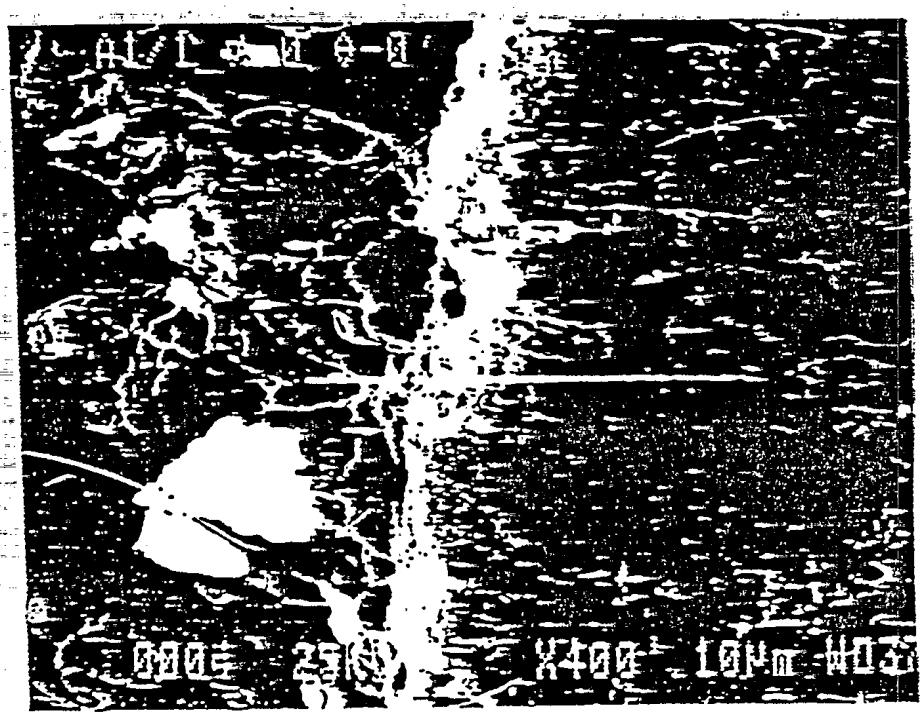

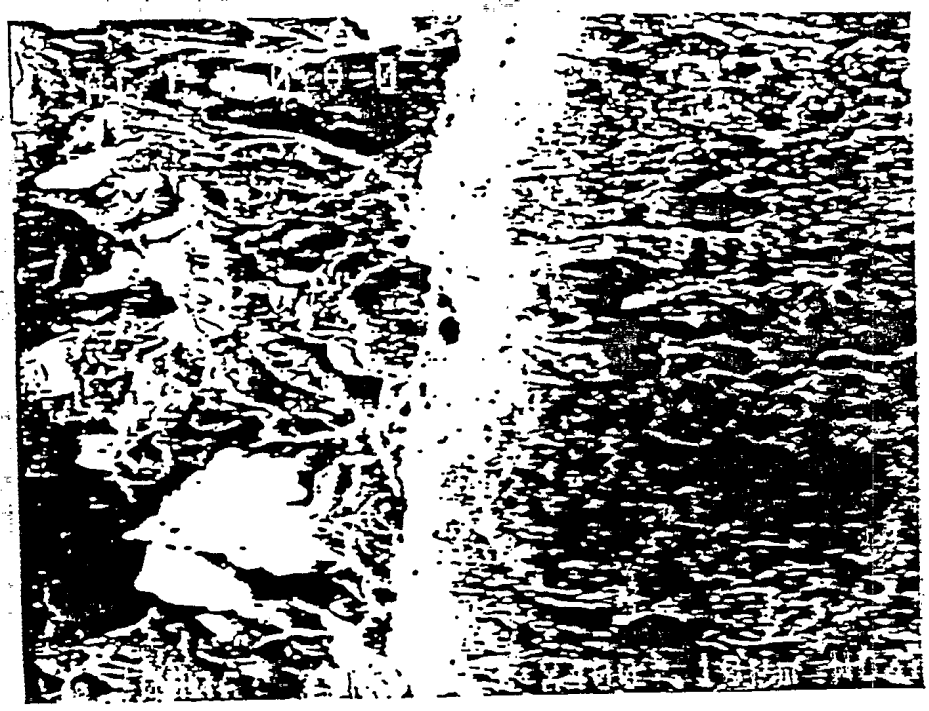

FIG.16: Typical stretch zone micrographs.

Table 1

Average Stretch Zone Width
Using 9-point and 3-point Averaging Techniques

	Samples			
Positions	SHB1	SHB2	SHB4	SHB6
1	108	100	105	36
2	109	64	103	35
3	99	104	102	48
4	103	91	101	59
5	95	79	105	60
6	97	96	104	66
7	96	93	111	90
8	82	78	120	95
9	98	95	104	106
9-point average	98	88	106	66
3-point average	98	89	103	62

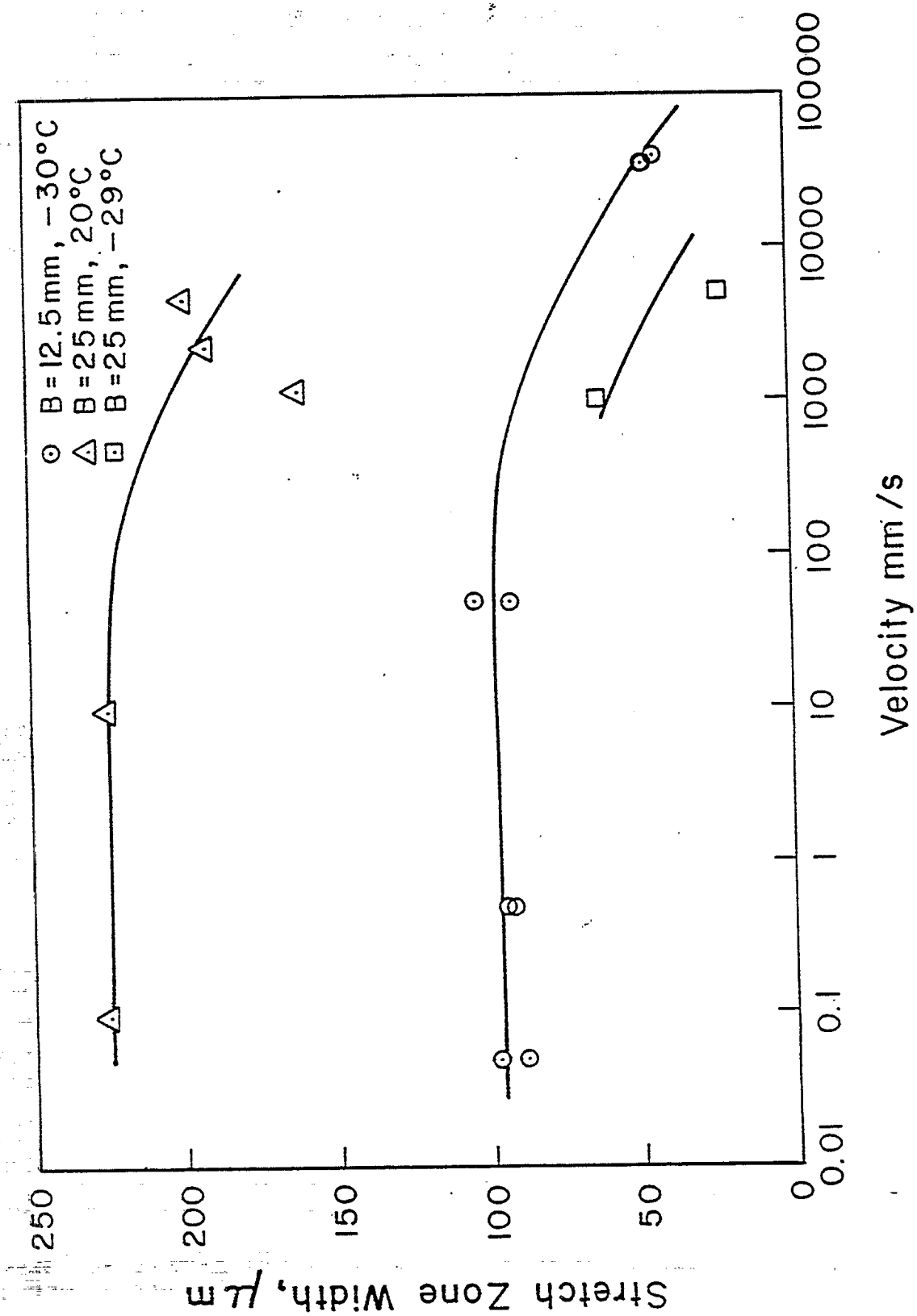
B=12.5mm, −30°C
B=25mm, 20°C
B=25mm, −29°C
Stretch Zone Width, μm
250
200
150
100
50
0
0.01
0.1
1
10
100
1000
10000
100000
Velocity mm/s

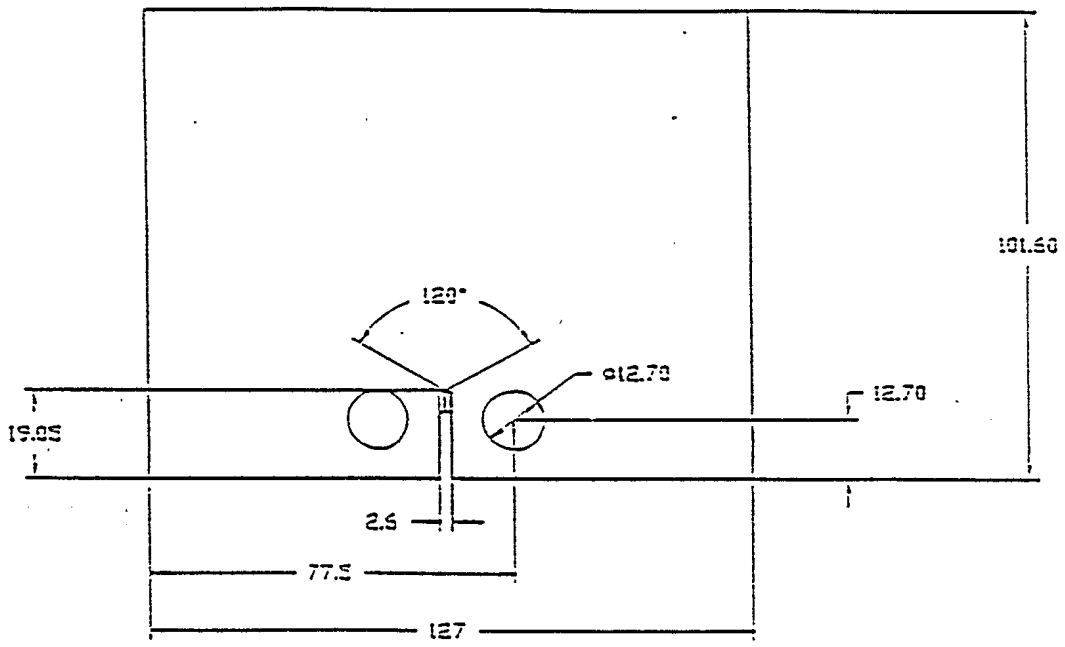

FIG.2: Initial sample to produce fatigued surface.

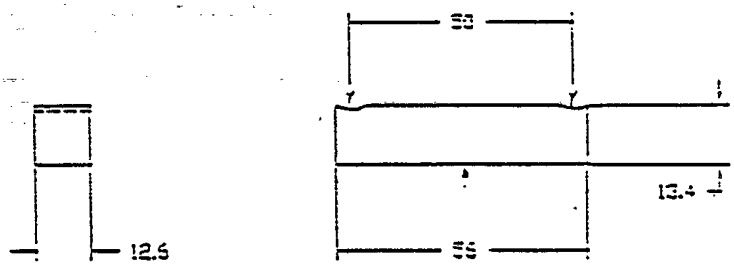

FIG.3: Final sample for bending test.

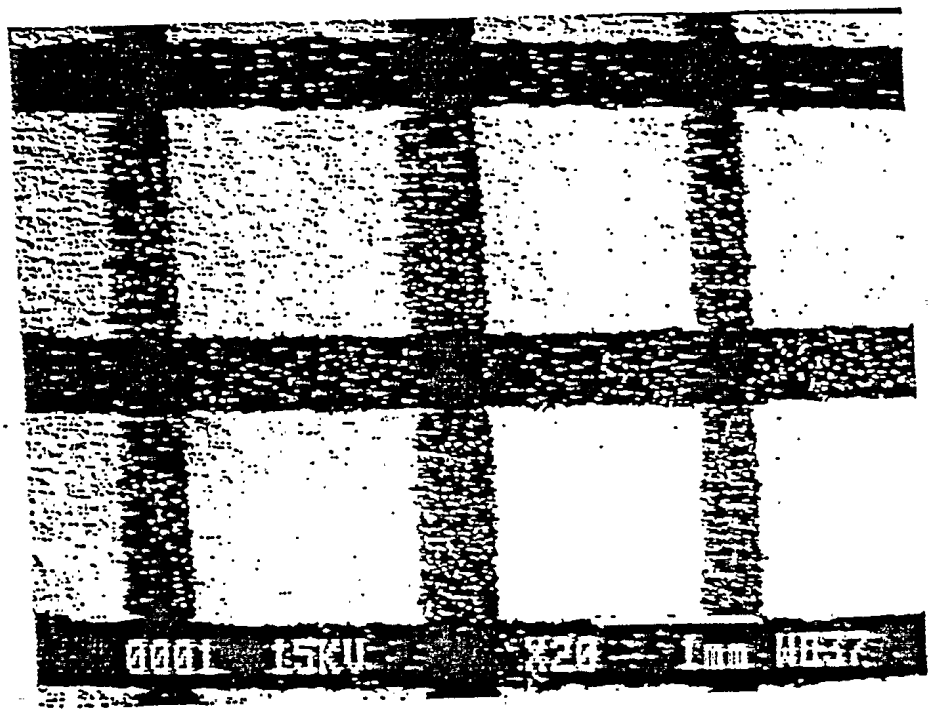

FIG.4: Grids of the fatigued surface of the specimen.

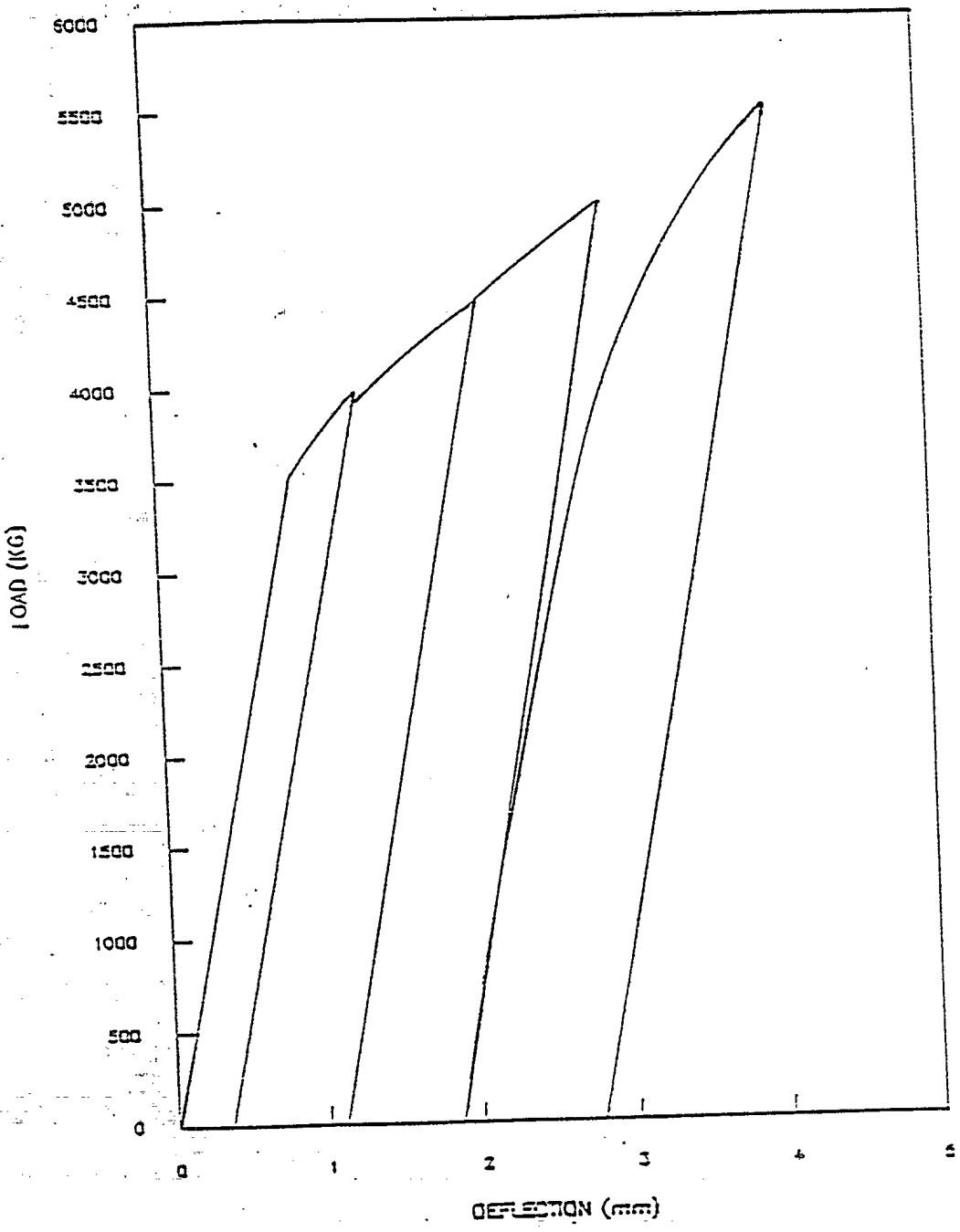

FIG.5: Load-displacement curve of the polished sample.

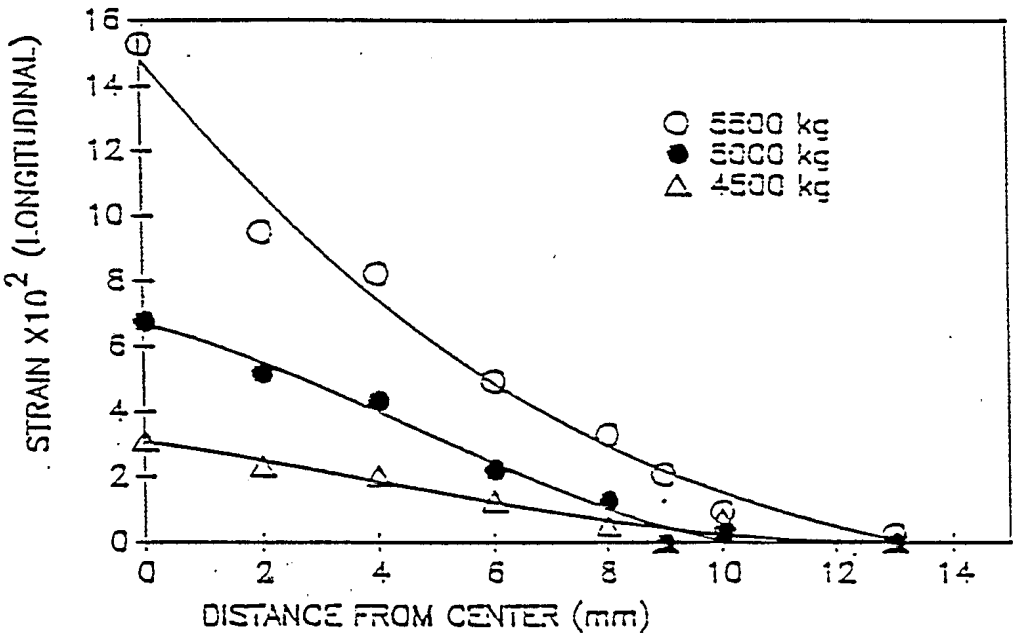

FIG.7: Longitudinal strain of the fatigued fractured sample.

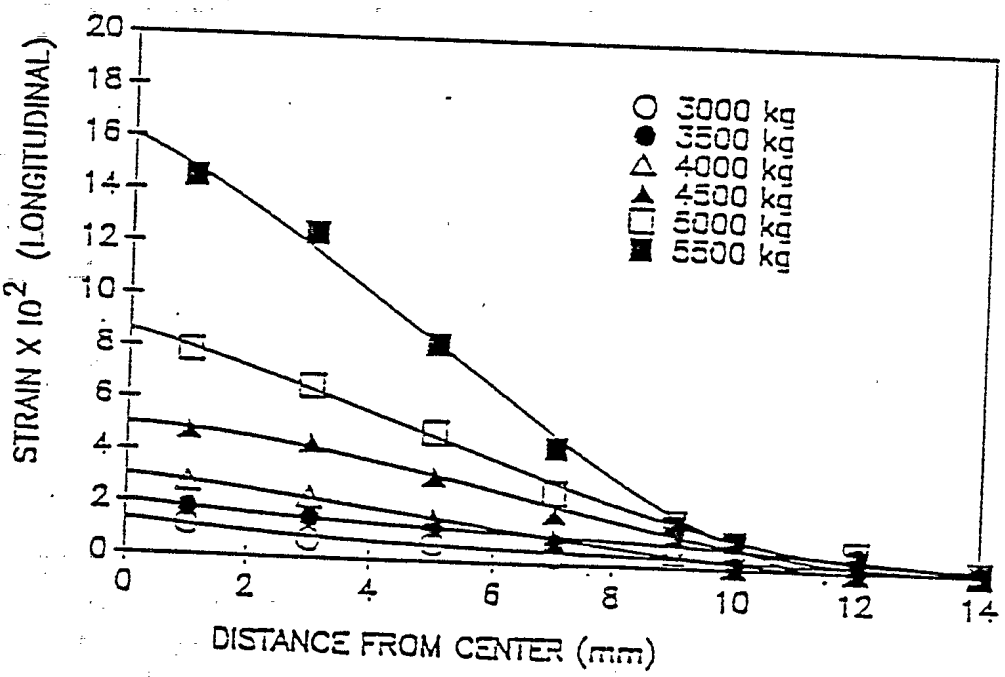

FIG.8: Longitudinal strain of the polished surface sample.

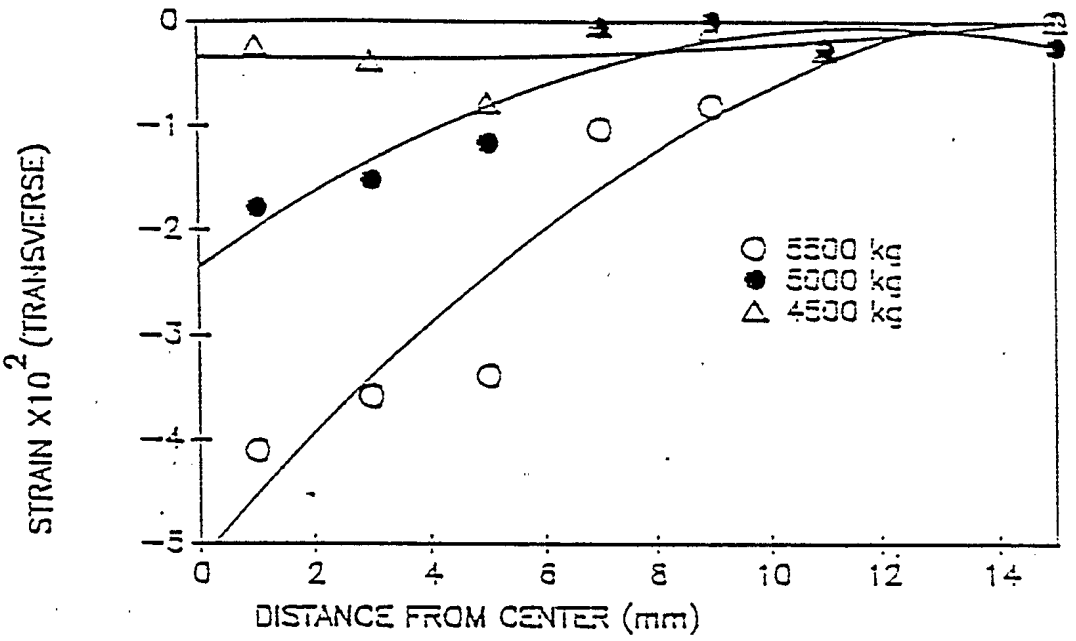

FIG.9: Transverse strain across the fatigue fractured surface.

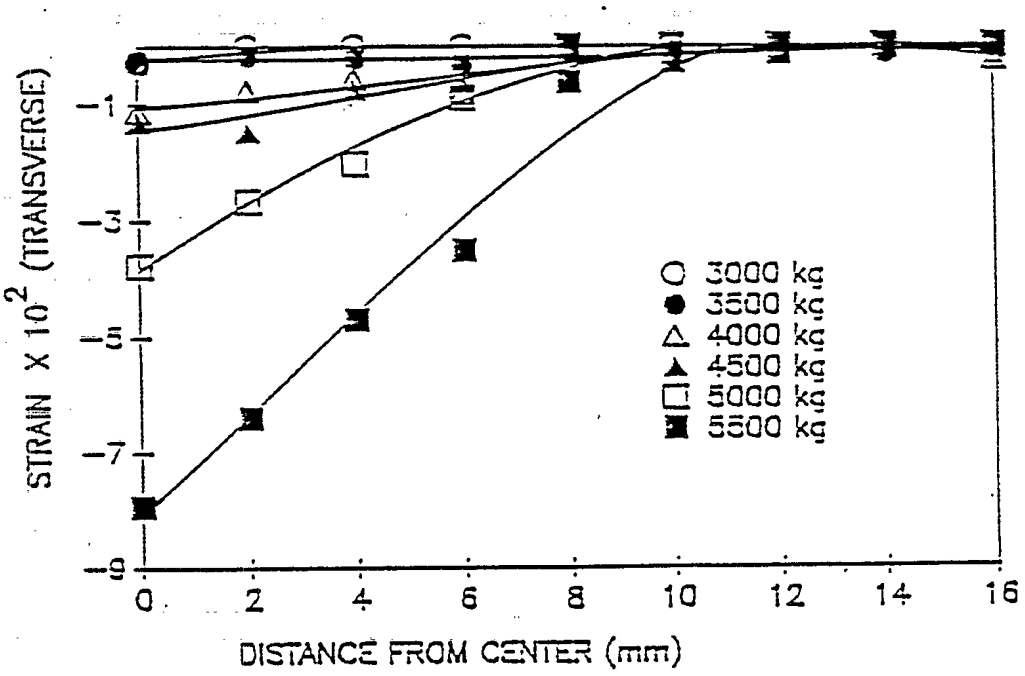

FIG.10: Transverse strain across the polished surface sample

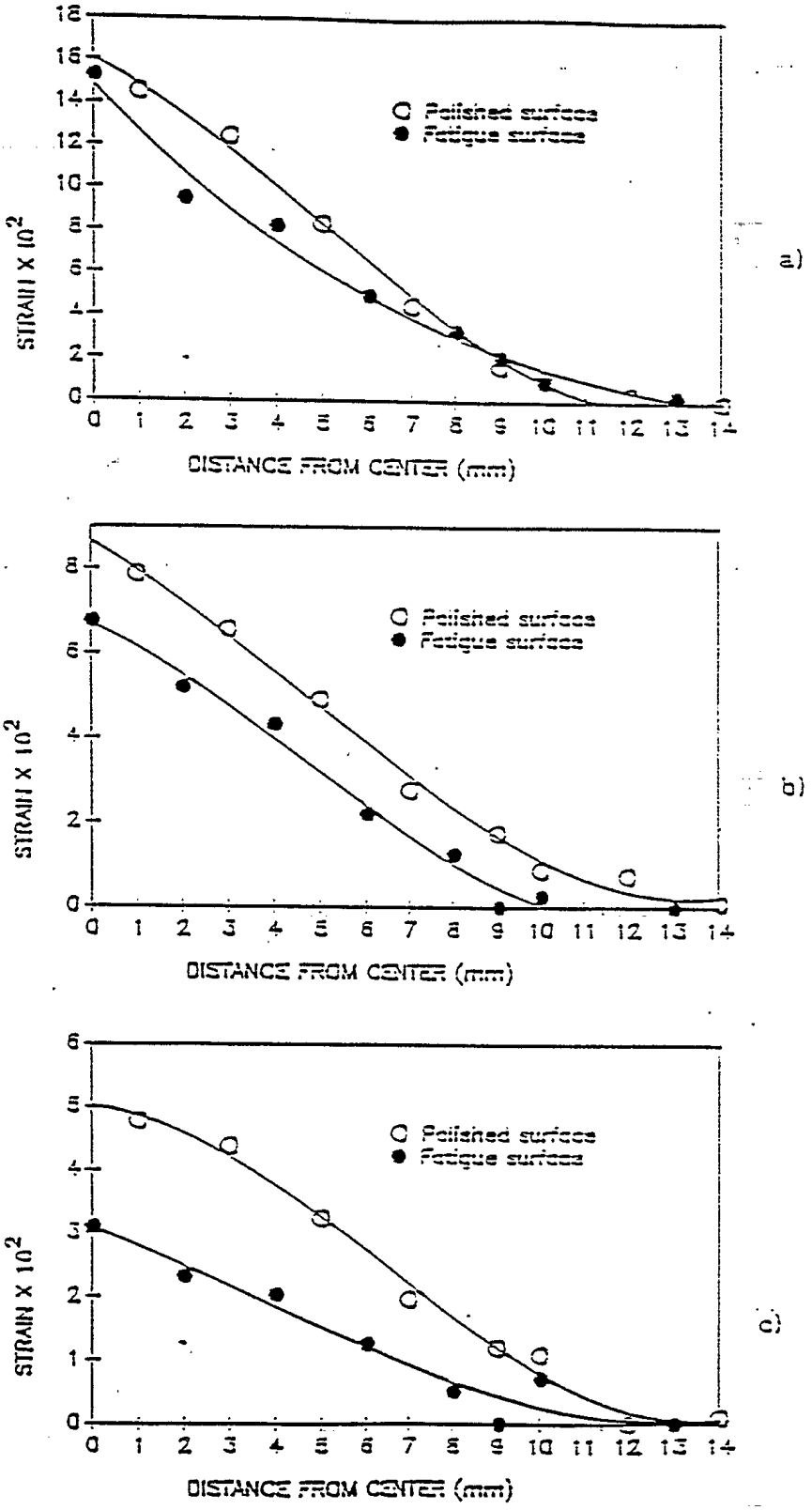

FIG.11: Comparison of the strains along the samples for two fatigue fractured and polished specimens for a) 4500 kg, b) 5000 kg and c) 5500 kg.

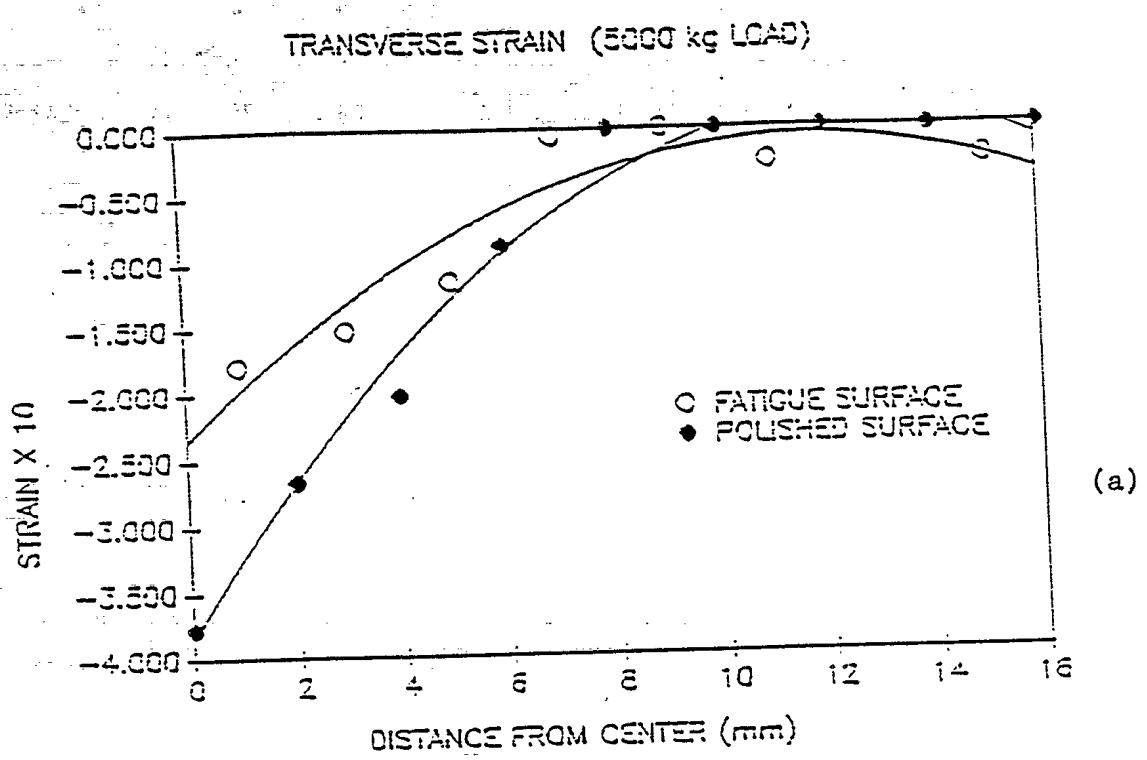

(a)

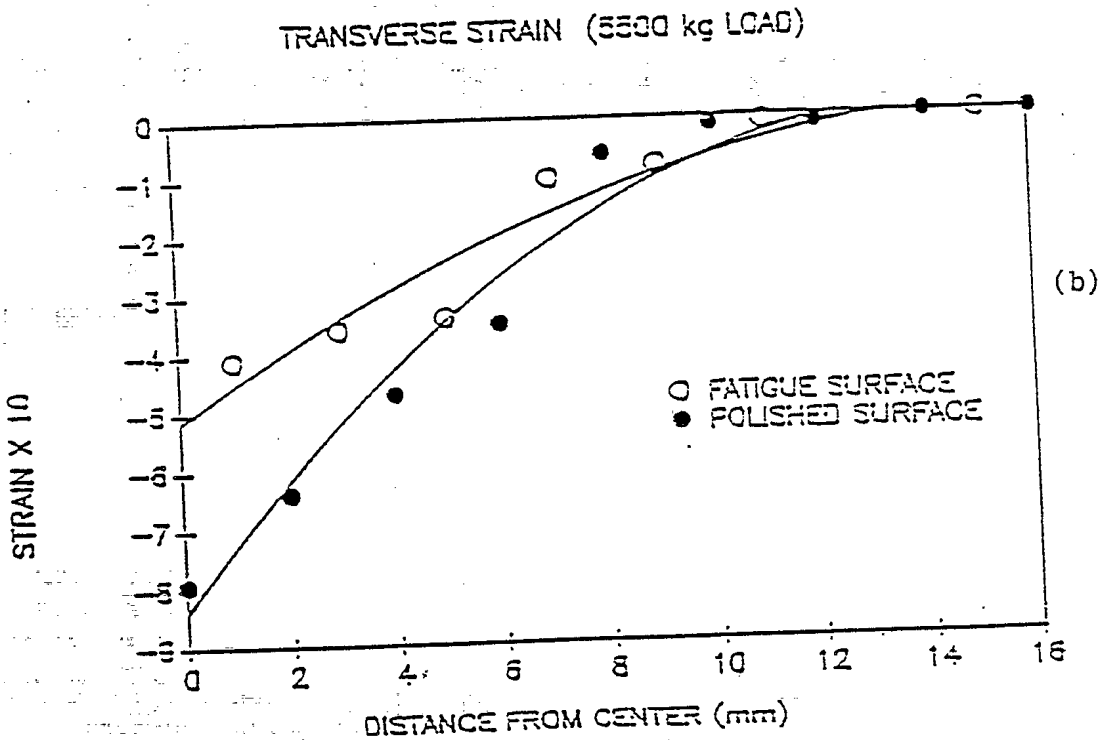

(b)

FIG.12: Comparison of the strains across the samples for fatigue fractured and polished surface specimens for a) 5000 kg. and b) 5500 kg.

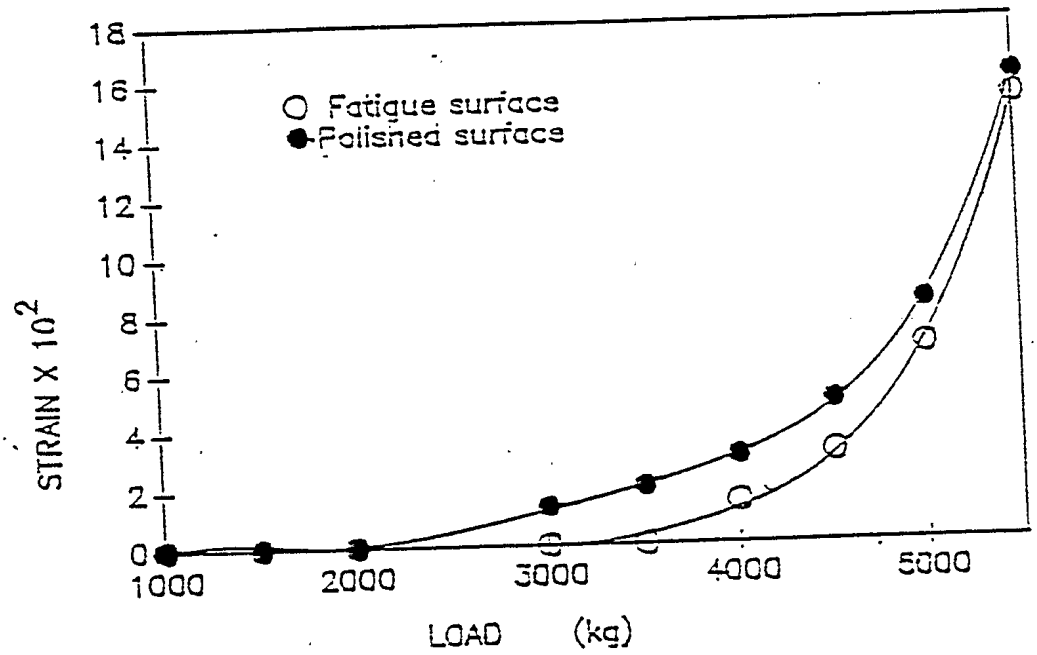

FIG.13: Maximum longitudinal strain at the middle of the sample versus applied load.

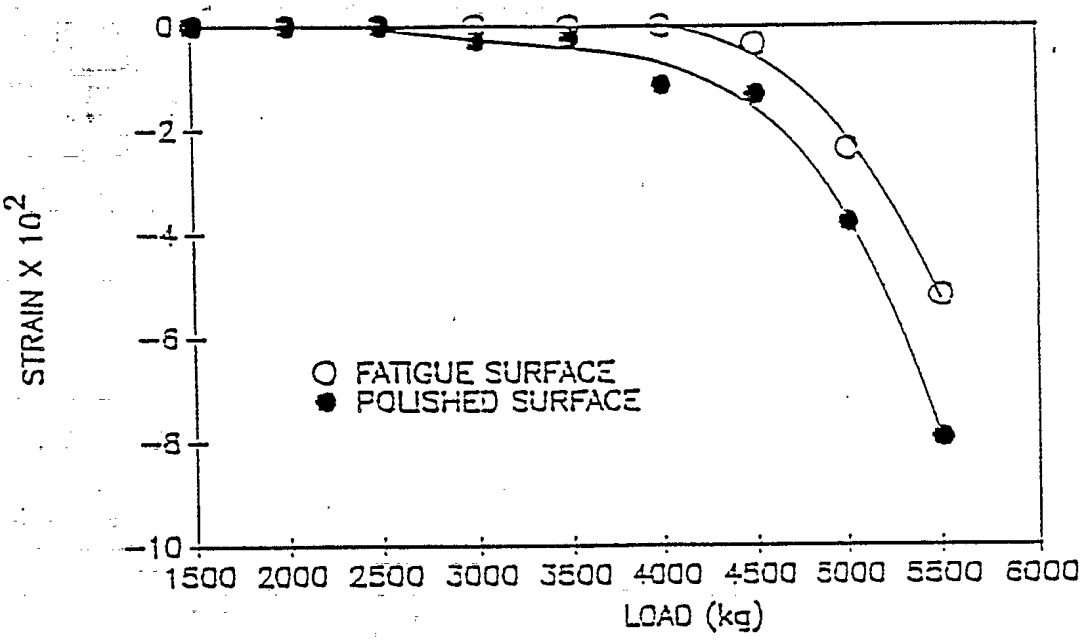

FIG.14: Maximun transverse strain at the middle of the sample versus applied load.

Where k is the strength coefficient and n is the strain hardening coefficient. Assuming that the stresses are the same for both fatigue surfaced and polished surfaced specimens and combining the experimental results for strains with calculated stresses, the bending tensile stress versus strain for both specimens is given in Figure 8. From this graph, σ_{y2} i.e. the yield point on the fatigue fractured surface, can be estimated. Since the stretch zone deformation is also a fatigue surface, the starting stress for deformation of this zone should also be the same. In other words, the stretch zone starting point occurs when the stress reaches σ_{y2}.

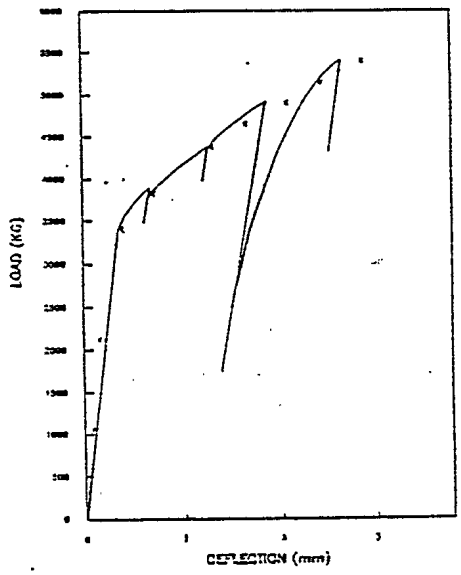

Fig. 6: Load- displacement curve of the polished specimen.

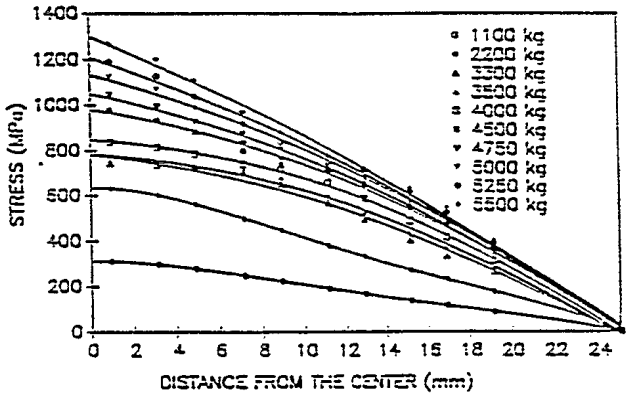

Fig. 7: Calculated Stress along the specimen by Finite element program.

In high strain rate experiments by Hyatt and Matthews (1990) the stretch zone width was measured for the J values below the critical value required for stable cracking. Figure 9 shows the linear function of the stretch zone width with J value below J_{1C}. The crack blunting theory assumes no deformation around the crack prior to loading the specimen. However Figure 9 shows that J is not zero at zero stretch zone width and the area around the crack tip is strain hardened prior to loading. The results agree that about 15% higher stress is required to start the deformation on a fatigue surface as shown in Figure 8.

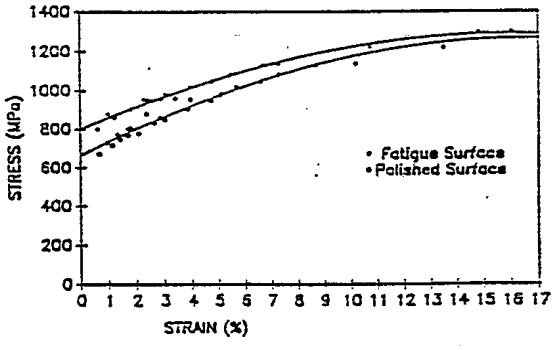

Fig. 8: Stress-Strain Curves for two fatigue surfaced and polished specimens resulted from bending test.

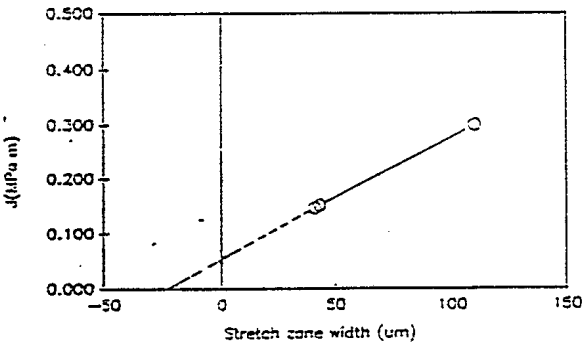

Fig. 9: Variation of stretch zone width with J.

Conclusions

The program showed that there is considerable merit in using the stretch zone width measurement as a procedure for evaluation of the fracture toughness of ductile submarine hull steels particularly at high loading rates where it is not feasible to perform compliance measurements. A better understanding of the Stretch Zone was obtained by studying its deformation characteristics and the role of fatigue predeformation on its development.